

# Magnetic and quantum disordered phases in triangular-lattice Heisenberg antiferromagnets

L. O. Manuel and H. A. Ceccatto

*Instituto de Física Rosario, Consejo Nacional de Investigaciones Científicas y Técnicas  
and Universidad Nacional de Rosario, Bvd. 27 de Febrero 210 Bis, 2000 Rosario, República Argentina*

We study, within the Schwinger-boson approach, the ground-state structure of two Heisenberg antiferromagnets on the triangular lattice: the  $J_1$ - $J_2$  model, which includes a next-nearest-neighbor coupling  $J_2$ , and the spatially-anisotropic  $J_1$ - $J'_1$  model, in which the nearest-neighbor coupling takes a different value  $J'_1$  along one of the bond directions. The motivations for the study of these systems range from general theoretical questions concerning frustrated quantum spin models to the concrete description of the insulating phase of some layered molecular crystals. For both models, the inclusion of one-loop corrections to saddle-point results leads to the prediction of nonmagnetic phases for particular values of the parameters  $J_1/J_2$  and  $J'_1/J_1$ . In the case of the  $J_1$ - $J_2$  model we shed light on the existence of such disordered quantum state, a question which is controversial in the literature. For the  $J_1$ - $J'_1$  model our results for the ground-state energy, quantum renormalization of the pitch in the spiral phase, and the location of the nonmagnetic phases, nicely agree with series expansions predictions.

## I. INTRODUCTION

The triangular-lattice Heisenberg antiferromagnet (TLHA) has played a fundamental role in the understanding of frustrated quantum spin systems. In particular, the existence of a nonmagnetic ground state in the  $S = 1/2$  system has been strongly debated in the literature, although there is now a widespread conviction that it displays the classical  $120^\circ$  spiral order.<sup>1,2</sup> In the last years, this particular problem was linked to more general questions concerning spin-liquid states and their possible connections to high- $T_c$  superconductivity. In this context, the most studied model has been the square-lattice Heisenberg antiferromagnet with first- and second-neighbor interactions, the so-called  $J_1$ - $J_2$  model.<sup>3</sup> The introduction of frustrating second-neighbor interactions leads, at intermediate values of the couplings, to the existence of a disordered spin-liquid state which intervenes between the Néel and "striped" (ferromagnetic in one direction, antiferromagnetic in the other) magnetic orders. This situation is by now fairly well established by a variety of numerical and analytical methods.<sup>3,4</sup> On the other hand, an extension of the TLHA including second-neighbor interactions, the  $J_1$ - $J_2$  TLHA, has also been considered.<sup>5-11</sup> This extension is a natural development after the thorough investigation of the model on the square lattice, but the existence or not of an intermediate spin-liquid phase in this case is not so clear, with most works favoring the non-existence of such a state.<sup>8-11</sup> This is somehow paradoxical, since the TLHA was considered for many years the best candidate to have a spin-liquid ground state just on the basis of the frustrating lattice topology. One would expect that the introduction of additional frustration through the  $J_2$  interaction should contribute to melt the already weak order of the nearest-neighbor model.

The study of the  $J_1$ - $J_2$  TLHA was mostly driven by purely theoretical motivations. On the other hand, recent experimental results have produced a surge of interest<sup>12-14</sup> in the ground-state properties of the nearest-neighbor TLHA with spatially anisotropic couplings:  $J_1$  along two bond directions and  $J'_1$  in the third one. It has been argued<sup>12</sup> that this model should describe the magnetic phases of the quasi-two-dimensional organic superconductors  $\kappa$ -(BEDT-TTF)<sub>2</sub>X. For these layered molecular crystals the relevant values of  $J'_1/J_1$  are around 0.3 - 1.0, with the ratio varying with the anion X and with uniaxial stress along the layer diagonal.

We have previously performed a study of both the  $J_1$ - $J_2$  and  $J_1$ - $J'_1$  TLHA using the rotational invariant Schwinger-boson approach (SBA) in a mean-field approximation.<sup>9</sup> At that time, our motivations for studying the latter model was the natural interpolation that it provides between the nearest-neighbor TLHA ( $J'_1 = J_1$ ) and the square-lattice antiferromagnet ( $J'_1 = 0$ ). We obtained a good agreement between the ground-state energy predicted in our approach and exact numerical values on finite lattices. Furthermore, no indication of a disordered state was found for the values of  $J_2/J_1$  and  $J'_1/J_1$  of interest. In this work we extend the calculations in<sup>9</sup> to include one-loop corrections to the mean-field picture. We have shown<sup>4,15</sup> that these corrections bring the saddle-point results in line with exact diagonalization values on finite clusters, which lends support to the SBA predictions for the thermodynamic limit. In particular, for the square-lattice  $J_1$ - $J_2$  model we found that there is a quantum nonmagnetic phase for  $0.53 \lesssim J_2/J_1 \lesssim 0.64$ . This result was obtained by considering the spin stiffness on large lattices and extrapolating to the thermodynamic limit, a procedure that avoids the infinite-lattice infrared divergencies associated to Bose condensation. We show here that similar behaviors are predicted for both the  $J_1$ - $J_2$  and  $J_1$ - $J'_1$  TLHA.

## II. THE CALCULATIONAL METHOD

We consider a general Hamiltonian of the form

$$H = \frac{1}{2} \sum_{\mathbf{r}, \mathbf{r}'} J(\mathbf{r} - \mathbf{r}') \vec{S}_{\mathbf{r}} \cdot \vec{S}_{\mathbf{r}'}, \quad (1)$$

where  $\mathbf{r}, \mathbf{r}'$  indicate sites on a triangular lattice. As usual, we write spin operators in terms of Schwinger bosons:<sup>16</sup>  $\vec{S}_i = \frac{1}{2} \mathbf{a}_i^\dagger \cdot \vec{\sigma} \cdot \mathbf{a}_i$ , where  $\mathbf{a}_i^\dagger = (a_{i\uparrow}^\dagger, a_{i\downarrow}^\dagger)$  is a bosonic spinor,  $\vec{\sigma}$  is the vector of Pauli matrices, and there is a boson-number restriction  $\sum_{\sigma} a_{i\sigma}^\dagger a_{i\sigma} = 2S$  on each site. With this representation the spin-spin interaction can be written as  $\vec{S}_i \cdot \vec{S}_j =: B_{ij}^\dagger B_{ij} : - A_{ij}^\dagger A_{ij}$ , where we defined the  $SU(2)$ -invariant order parameters  $A_{ij} = \frac{1}{2} \sum_{\sigma} \sigma a_{i\sigma} a_{j\bar{\sigma}}$  and  $B_{ij}^\dagger = \frac{1}{2} \sum_{\sigma} a_{i\sigma}^\dagger a_{j\sigma}$  ( $\bar{\sigma} = -\sigma$ ,  $\sigma = \pm 1$ ), and the notation  $:O:$  indicates the normal order of operator  $O$ . Thus, we can formulate the partition function for the Hamiltonian (1) as a functional integral over boson coherent states, which allows its evaluation by a saddle-point expansion. Since the theory presents a local  $U(1)$  symmetry, we use collective coordinate methods —as developed in the context of relativistic lattice gauge theories<sup>17</sup>— to handle the infinitely-many zero modes associated to the symmetry breaking in the saddle point. These modes without restoring forces, which correspond to local gauge transformations, are eliminated by the exact integration of the collective coordinates. Such a program can be carried out by enforcing in the functional integral measure the so-called background gauge condition, or “natural” gauge,<sup>17</sup> by means of the Fadeev-Popoff trick. In this way we restrict the integrations in the partition function to field fluctuations that are orthogonal to the collective coordinates. At  $T = 0$ , after carrying out the integrations on these genuine fluctuations, we obtain the one-loop correction to the ground-state energy *per site*,

$$E_1 = -\frac{1}{2\pi} \int_{-\infty}^{\infty} d\omega \sum_{\mathbf{k}} \ln \left( \frac{\Delta_{\text{FP}}(\mathbf{k}, \omega)}{|\omega| \sqrt{\det \mathcal{A}_{\perp}^{(2)}(\mathbf{k}, \omega)}} \right). \quad (2)$$

Here the Fadeev-Popoff determinant  $\Delta_{\text{FP}}(\mathbf{k}, \omega) = |\vec{\varphi}_0^L(\mathbf{k}, \omega) \cdot \vec{\varphi}_0^R(\mathbf{k}, \omega)|$ , where  $\vec{\varphi}_0^L(\mathbf{k}, \omega)$  is the *left* zero mode of the dynamical matrix  $\mathcal{A}^{(2)}$  in the  $\mathbf{k}-\omega$  subspace, and  $\mathcal{A}_{\perp}^{(2)}$  is the projection of this matrix in the subspace orthogonal to the collective coordinates. The dynamical matrix  $\mathcal{A}^{(2)}$  is the Hessian of the effective action as a function of the decoupling (Hubbard-Stratonovich) fields (see<sup>4</sup> for details).

In the ordered phases of the model the Bose condensate breaks the global  $SU(2)$  symmetry and its density gives the local magnetization.<sup>16</sup> The associated physical Goldstone modes at  $\mathbf{k} = 0, \pm \mathbf{Q}$  ( $\mathbf{Q}$  is the magnetic wavevector) lead to serious infrared divergencies of intermediate quantities, which have to be cured by standard renormalization prescriptions. In order to avoid these problems we have computed physical quantities (which are free of divergencies) on large by finite lattices, and finally extrapolated these values to the thermodynamic limit. We considered clusters with the spatial symmetries of the infinite triangular lattice, corresponding to translation vectors  $\mathbf{T}_1 = (n+m)\mathbf{e}_1 + m\mathbf{e}_2$ ,  $\mathbf{T}_2 = n\mathbf{e}_1 + (n+m)\mathbf{e}_2$ .<sup>18,19</sup> Here  $\mathbf{e}_1 = (a, 0)$  and  $\mathbf{e}_2 = (-\frac{1}{2}a, \frac{\sqrt{3}}{2}a)$  are the basic triangular lattice vectors. To fit to the cluster shapes the expected (spiral) magnetic orders, and also to allow the calculation of the stiffness, we impose arbitrary boundary conditions  $\vec{S}_{\mathbf{r}+\mathbf{T}_i} = \mathcal{R}_{\hat{n}}(\Phi_i) \vec{S}_{\mathbf{r}}$  ( $i = 1, 2$ ), where  $\mathcal{R}_{\hat{n}}(\Phi_i)$  is the matrix that rotates an angle  $\Phi_i$  around some axis  $\hat{n}$  (notice that we are using boldface (arrows) for vectors in real (spin) space). It is convenient to perform local rotations  $\vec{S}_{\mathbf{r}} \rightarrow \mathcal{R}_{\hat{n}}(\theta_{\mathbf{r}}) \vec{S}_{\mathbf{r}}$  of angle  $\theta_{\mathbf{r}} = \Delta \mathbf{Q} \cdot \mathbf{r}$ , so that with the choice  $\Delta \mathbf{Q} \cdot \mathbf{T}_i = \Phi_i$  the boundary conditions become the standard periodic ones  $\vec{S}_{\mathbf{r}+\mathbf{T}_i} = \vec{S}_{\mathbf{r}}$ . Then, we define the ( $T = 0$ ) stiffness tensor  $\rho_n^{\hat{z}}$  by

$$\rho_n^{\hat{z}} = \left. \frac{\partial^2 E_{\text{GS}}(\mathbf{Q} + \Delta \mathbf{Q})}{\partial \theta_i \partial \theta_j} \right|_{\Delta \mathbf{Q} = 0}, \quad (3)$$

where  $E_{\text{GS}}$  is the ground-state energy *per spin* and  $\theta_i = \Delta \mathbf{Q} \cdot \mathbf{e}_i$  ( $i = 1, 2$ ) are the twist angles along the basis vectors  $\mathbf{e}_i$ . In the next two sections we will apply this formalism to the models under consideration.

## III. THE $J_1 - J_2$ TLHA

The  $J_1 - J_2$  TLHA is given by (1) with  $J(\mathbf{r} - \mathbf{r}') = J_1(J_2)$  for  $\mathbf{r}$  and  $\mathbf{r}'$  nearest (next-nearest) neighbor sites, and 0 otherwise. For classical spin vectors, when  $\alpha \equiv J_2/J_1 < 1/8$  the lowest-energy configuration in this model is the

commensurate spiral with magnetic wavevector  $\mathbf{Q} = (\frac{4\pi}{3a}, 0)$ ; for  $1/8 < \alpha < 1$  there is a degeneracy between the two-sublattice and four-sublattice Néel orders. Quantum fluctuations lift this degeneracy and select, through an "order from disorder" phenomenon, the two-sublattice collinear ground-state with magnetic wavevector  $\mathbf{Q} = (\frac{\pi}{a}, -\frac{\pi}{\sqrt{3}a})$ . This scenario was first proposed using spin-wave theory<sup>8</sup> and later confirmed by a study of the thermodynamic-limit collapse to the ground state of low lying levels.<sup>11</sup> The correction (2) to the saddle-point value  $E_0$  leads to the ground-state energy  $E_{\text{GS}} = E_0 + E_1$  shown in Fig. 1. This figure contains the result for the infinite lattice and also for a finite cluster of 12 sites, which allows a comparison with exact results obtained by numerical diagonalization.<sup>6</sup> We see that the addition of the Gaussian correction  $E_1$  improves the saddle-point value  $E_0$ , particularly for the  $120^\circ$  spiral phase. Moreover, the departure of the fluctuation-corrected results from the exact values in the range  $0.1 \lesssim \alpha \lesssim 0.2$  hints to the possible existence of a disordered phase in this region. In the thermodynamic limit, at saddle-point order the theory predicts a first order transition between the two magnetic ground states at some intermediate frustration  $\alpha \simeq 0.16$ , with no intervening disordered phase.<sup>9</sup> After the inclusion of the Gaussian fluctuations there is a window  $0.12 \lesssim \alpha \lesssim 0.19$  where the stiffness vanishes (see below) and the magnetic order is melted by the combined action of quantum fluctuations and frustration. This result should be compared with the linear spin wave results of<sup>7</sup>, which predict a quantum nonmagnetic phase in the range  $(0.1, 0.14)$ . Notice, however, that within spin-wave theory this window closes when corrections to the leading-order calculations are included.<sup>8</sup> We stress that the same happens in this approach for the  $J_1 - J_2$  model on the square lattice, where however other methods confirm the existence of a nonclassical phase.

As stated above, the existence or not of magnetic long-range order in the thermodynamic limit was investigated by considering the spin-stiffness tensor (3).<sup>20</sup> For spins lying on the  $xy$ -plane, it is necessary to consider both the parallel stiffness  $\rho_{\parallel} \equiv \rho_{\hat{z}}$  under a twist around  $\hat{z}$  and the perpendicular stiffness  $\rho_{\perp} \equiv \bar{\rho}_{xy}$  for twists around an arbitrary versor  $\hat{n}$  on this plane. However, on clusters with periodic boundary conditions our approach is rotational invariant and we only have access to  $\bar{\rho} = \frac{1}{3}(\rho_{\parallel} + 2\rho_{\perp})$ . On the other hand, we found that the large- $S$  Schwinger-boson prediction for this quantity is exactly  $4/3$  smaller than the corresponding classical result. As discussed in<sup>15</sup>, to solve these problems we considered clusters that fit the magnetic orders in the  $xy$ -plane with appropriate twisted boundary conditions.<sup>18,19</sup> In this case, since the rotational invariance is explicitly broken by the boundary conditions, one is able to compute the parallel stiffness  $\rho_{\parallel}$  and, moreover, the large- $S$  predictions have the correct behavior (no *ad hoc* factors are required to correct this quantity).<sup>15</sup> Finally, using the values for  $\bar{\rho}$  obtained from clusters with periodic boundary conditions it is possible to determine  $\rho_{\perp} \equiv \frac{3}{2}\bar{\rho} - \frac{1}{2}\rho_{\parallel}$ . The corresponding results are presented in Fig. 2, both at saddle-point and one-loop orders for comparison. Notice that in the  $120^\circ$  spiral phase  $\rho_{\parallel}$  softens first than  $\rho_{\perp}$ , while the behavior is the opposite for the collinear state. Since the indirect calculation of  $\rho_{\perp}$  requires the use of *ad hoc* factors to renormalize  $\bar{\rho}$ , the determination of the upper limit for the disordered phase might be unreliable. However, based on our previous experience with the SBA, we believe the existence of an intermediate nonmagnetic phase can be trusted.

#### IV. THE $J_1 - J'_1$ TLHA

For the  $J_1 - J'_1$  TLHA, in (1) we take  $J(\mathbf{r} - \mathbf{r}') = J_1$  for  $\mathbf{r} - \mathbf{r}' = \mathbf{e}_i$  ( $i = 1, 2$ ) and  $J(\mathbf{r} - \mathbf{r}') = J'_1$  for  $\mathbf{r} - \mathbf{r}' = \mathbf{e}_3 \equiv \mathbf{e}_1 + \mathbf{e}_2$ . As mentioned above, this model is interesting in view of its connections to the spin degrees of freedom in the insulating phase of some layered organic superconductors.<sup>12</sup> Very recent works have investigated its ground-state phase diagram and other properties, using spin-wave theory<sup>13</sup> and series expansions.<sup>14</sup> For classical vectors, with  $\eta \equiv J'_1/J_1 < 1/2$  the lowest-energy configuration is the two-sublattice Néel order discussed in the previous section, with the (frustrated) ferromagnetic arrangement of the spins along the weakly-coupled  $\mathbf{e}_3$  direction. For  $\eta > 1/2$  the preferred spin configuration becomes an incommensurate spiral, with the angle  $Q_{\text{Class}}$  between neighboring spins along the  $\mathbf{e}_1, \mathbf{e}_2$  directions given by  $Q_{\text{Class}} = \arccos(-\frac{1}{2\eta})$ .

The inclusion of the quantum nature of spins by means of the SBA produces the results for the ground-state energy shown in Fig. 3. In this figure we give the mean-field values and the fluctuation-corrected results, and compare them with the series expansion predictions from<sup>14</sup>. We see that the fluctuations produce regions in which the saddle-point solutions become unstable. On the other hand, for those values of  $\eta$  where the magnetic phases considered are stable there is a very good agreement between both methods. It is also of interest to compare the quantum renormalization of the spiral pitch; in Fig. 4 we plot the classical result for  $Q$  given above, and the corresponding angle that minimize the quantum ground-state energy. Again, in the region where the magnetic phases are stable the results nicely agree with those coming from series expansions. Furthermore, we have checked at mean-field order that the angle that minimizes the total energy corresponds also to the minimum of the quasiparticle dispersion relation, a fact that was used in<sup>14</sup> to determine  $Q$ .

To establish the regions without magnetic order we studied again the spin-stiffness behavior. Like for classical vectors, the stiffness tensor (3) is diagonal in the (perpendicular) directions  $\mathbf{e}_3$  and  $\mathbf{e}_2 - \mathbf{e}_1$ ; the corresponding stiffness

along these directions are plotted in Fig. 5. We found a qualitatively different behavior between the saddle-point and one-loop results; most notably, in the Néel phase the Gaussian fluctuations soften first the classically stronger stiffness in the  $\mathbf{e}_3$  direction. At mean-field order our calculations indicate a continuous transition between the two magnetic phases at  $\eta \simeq 0.621$ , and the absence of a magnetic saddle-point solution beyond  $\eta \simeq 2.20$ . The corrected results show the melting of the Néel phase at  $\eta \simeq 0.61$ , still above the classical point  $\eta_{\text{Class}} = 1/2$ , and predict a disordered quantum phase in the range  $0.61 \lesssim \eta \lesssim 0.96$ . Furthermore, the incommensurate phase becomes stable only in a reduced parameter region  $0.96 \lesssim \eta \lesssim 1.10$ . In this case the instability appears as a negative eigenvalue of the projected dynamical matrix  $\mathcal{A}_\perp^{(2)}$  in (2). These results are in fair agreement with the series-expansion predictions from<sup>14</sup>, which indicate that the Néel order disappears at  $\eta \sim 0.65 - 0.7$ , the disorder region extends from this value up to  $\eta \sim 0.9$ , and there is an incommensurate phase for  $\eta \gtrsim 0.9$  with no clear ending point.

## V. CONCLUSIONS

In conclusion, we have considered, within the SBA, the Gaussian-fluctuation corrections to the spin stiffness of the  $J_1 - J_2$  and  $J_1 - J'_1$  TLHA. For the  $J_1 - J_2$  model we found that the order-parameter fluctuations weaken the stiffness, which is reduced by increasing the frustration until it vanishes leaving a small window  $0.12 \lesssim \alpha \lesssim 0.19$  where the system has no long-range magnetic order. Like in previous studies, we found that the consideration of clusters which require twisted boundary conditions to fit the magnetic orders avoids the use of *ad hoc* factors to correct the Schwinger-boson predictions. This fact points to a subtle interplay between rotational invariance and the relaxation of local constraints in this approach.

In the case of the  $J_1 - J'_1$  TLHA our results indicate a rich phase diagram, with at least two magnetic (Néel and incommensurate spiral) phases and two disordered quantum states in the parameter region of interest. One of the most notable aspects of our calculations is the quantum renormalization of the magnetic wavevector in the spiral phase, which agrees remarkably with the series expansion prediction. We also found that the Néel order extends beyond its classical stability point up to a value  $\eta \simeq 0.61$ , where it seems to melt continuously into a purely quantum phase. On the contrary, the spiral order is favored in a reduced parameter range, with our results indicating first order transitions from this phase to the nonmagnetic states. These first order transitions appear in our calculations as local instabilities against the order-parameter fluctuations.

Finally, there still remains the difficult task of characterizing the disordered quantum phases of the models under consideration. Some attempts in this direction have already been done, for both the  $J_1 - J_2$ <sup>5</sup> and  $J_1 - J'_1$ <sup>14</sup> TLHA, but there is not clear understanding of these phases yet. They are usually considered to be of the resonant-valence-bond type, and are in general described starting from a regular strong-bond (dimer) covering of the lattice.<sup>14</sup> These investigations can be performed within the formalism developed here, since the SBA does not rely on having magnetic order in the system like, for instance, spin-wave theory. However, these studies would require the extension of the present calculations to larger magnetic unit cells and the computation of physical quantities able to characterize the new phases, a question that is far from trivial.

## ACKNOWLEDGMENTS

We are grateful to Adolfo E. Trumper for useful discussions and for calling our attention to Ref. 12.

---

<sup>1</sup> D. A. Huse and V. Elser, Phys. Rev. Lett. **60**, 2531 (1988); B. Bernu, C. Lhuillier, and L. Pierre, Phys. Rev. Lett. **69**, 2590 (1992).

<sup>2</sup> L. Capriotti, A. Trumper, and S. Sorella, cond-mat/9901068 (to appear in Phys. Rev. Lett.).

<sup>3</sup> A. V. Dotsenko and O. P. Sushkov, Phys. Rev. B **50**, 13821 (1994) and references therein.

<sup>4</sup> A. E. Trumper, L. O. Manuel, C. J. Gazza, and H. A. Ceccatto, Phys. Rev. Lett. **78**, 2216 (1997).

<sup>5</sup> G. Baskaran, Phys. Rev. Lett. **63**, 2524 (1989).

<sup>6</sup> T. Jolicoeur, E. Dagotto, E. Gagliano, and S. Bacci, Phys. Rev. B **42**, 4800 (1990).

<sup>7</sup> N. B. Ivanov, Phys. Rev. B **47**, 9105 (1993).

<sup>8</sup> A. Chubukov and T. Jolicoeur, Phys. Rev. B **46**, 11137 (1992); S. E. Korshunov, Phys. Rev. B **47**, 6165 (1993).

- <sup>9</sup> C. J. Gazza and H. A. Ceccatto, *J. Condens. Matt.* **5**, L135 (1993).  
<sup>10</sup> R. Deutscher and H. U. Everts, *Z. Phys. B* **93**, 77 (1993).  
<sup>11</sup> P. Lecheminant, B. Bernu, C. Lhuillier, and L. Pierre, *Phys. Rev. B* **52**, 6647 (1995).  
<sup>12</sup> R. H. McKenzie, *Comments Cond. Mat. Phys.* **18**, 309 (1998).  
<sup>13</sup> A. E. Trumper, cond-mat/9812311; J. Merino, Ross H. McKenzie, J. B. Marston, and C. H. Chung, cond-mat/9812429 (to appear in *J. Phys.: Cond. Matter*).  
<sup>14</sup> Z. Weihong, R. H. McKenzie, and R. R. P. Singh, cond-mat/9812262 (to appear in *Phys. Rev. B*).  
<sup>15</sup> L. O. Manuel, A. E. Trumper, and H. A. Ceccatto, *Phys. Rev. B* **57**, 8348 (1998).  
<sup>16</sup> A. Auerbach, *Interacting Electrons and Quantum Magnetism*, Springer-Verlag New York, Inc. (1994).  
<sup>17</sup> J. L. Gervais and B. Sakita, *Phys. Rev. D* **11**, 2943 (1975); A. M. Polyakov, *Nucl. Phys. B* **120**, 429, (1977).  
<sup>18</sup> B. Bernu, P. Lecheminant, C. Lhuillier, and L. Pierre, *Phys. Rev. B* **50**, 10048 (1994).  
<sup>19</sup> P. Lecheminant, B. Bernu, C. Lhuillier, and L. Pierre, *Phys. Rev. B* **52**, 9162 (1995).  
<sup>20</sup> A. E. Feiguin, C. J. Gazza, A. E. Trumper, and H. A. Ceccatto, *Phys. Rev. B* **52**, 15053 (1995).

FIG. 1: Ground-state energy *per site*  $E_{GS}$  of the  $J_1 - J_2$  TLHA as a function of the frustration parameter  $\alpha = J_2/J_1$ . Dashed and full lines give the mean-field and fluctuation-corrected results, respectively. The lower curves correspond to the energy of a 12-site cluster (the values are shifted by -0.05 for clarity); the upper curves give the thermodynamic-limit results. Dots are exact numerical values from<sup>6</sup>.

FIG. 2: a) Parallel stiffness  $\rho_{\parallel}$ , and b) perpendicular stiffness  $\rho_{\perp}$  for the  $J_1 - J_2$  TLHA as a function of the frustration parameter  $\alpha$ . Dashed and full lines give the saddle-point and fluctuation-corrected results, respectively. The thin vertical lines separate the regions with magnetic order from the middle parameter range where there is a quantum disordered phase.

FIG. 3: Ground-state energy *per site*  $E_{GS}$  of the  $J_1 - J'_1$  TLHA as a function of  $\eta = J'_1/J_1$ . Dashed and full lines give the mean-field (MF) and fluctuation-corrected (FL) results, respectively. Dots are series expansion predictions from<sup>14</sup>.

FIG. 4: Relative angle  $Q$  between nearest-neighbor spins as a function of  $\eta$ . The thick full line corresponds to the lowest-energy configuration of classical spins, the dashed line is the mean-field prediction in the quantum case, and the thin full line is the series expansion result from<sup>14</sup>. Open dots are the fluctuation-corrected results in the incommensurate phase (shown in more detail in the inset).

FIG. 5: Spin stiffness  $\rho_{\parallel}$  for the  $J_1 - J'_1$  model as a function of  $\eta$ . Dashed and full lines correspond to saddle-point and fluctuation-corrected results, respectively. The thin vertical lines separate the regions with antiferromagnetic (AF) and incommensurate (INC) spiral orders from the parameter ranges corresponding to disordered quantum phases.

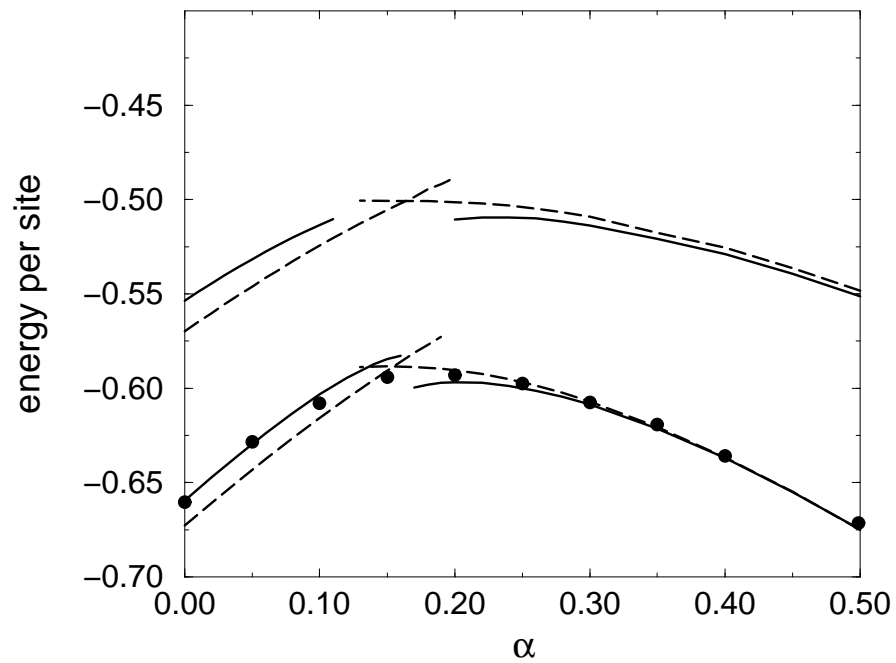


FIG. 1.

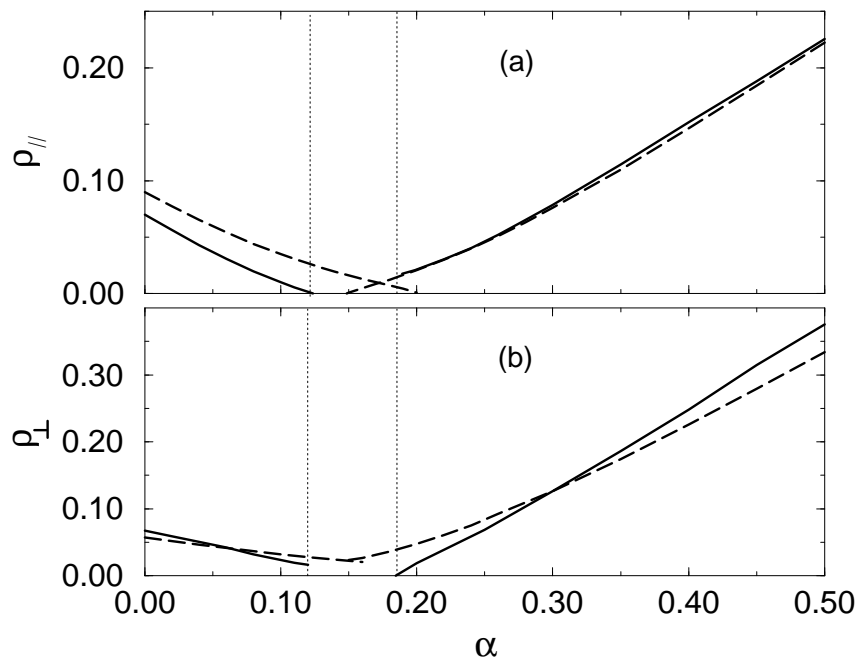


FIG. 2.

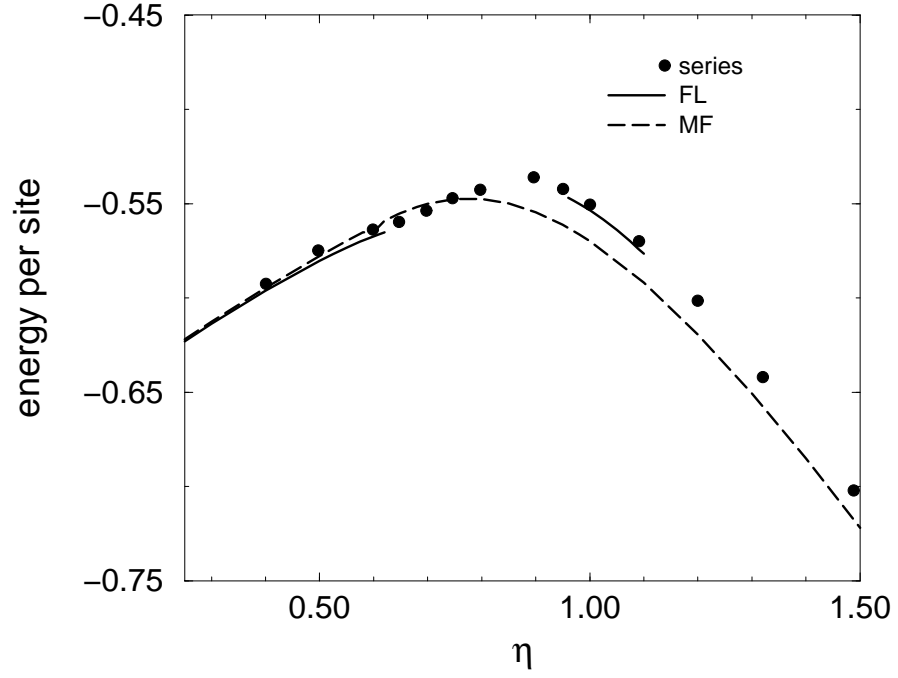


FIG. 3.

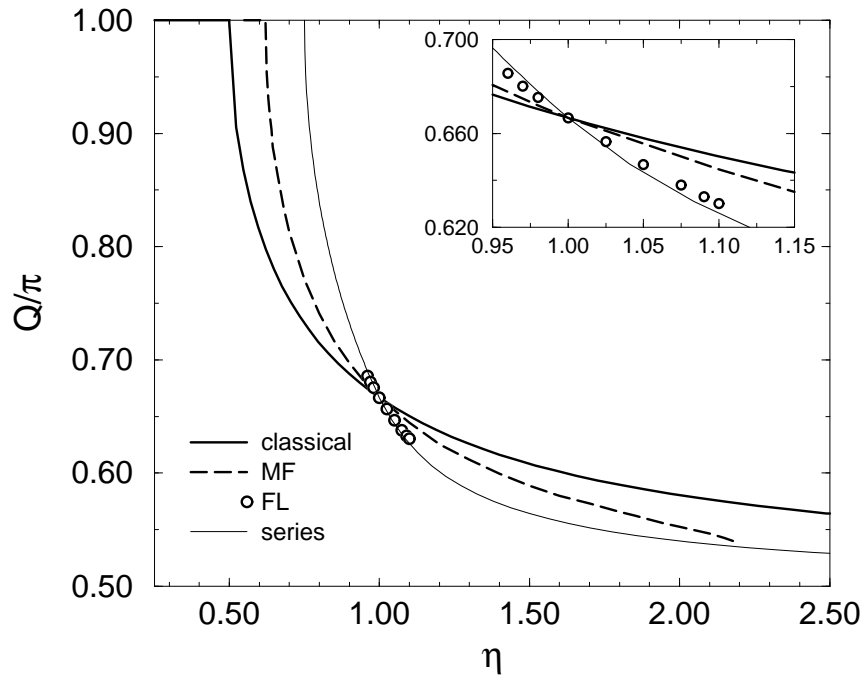


FIG. 4.

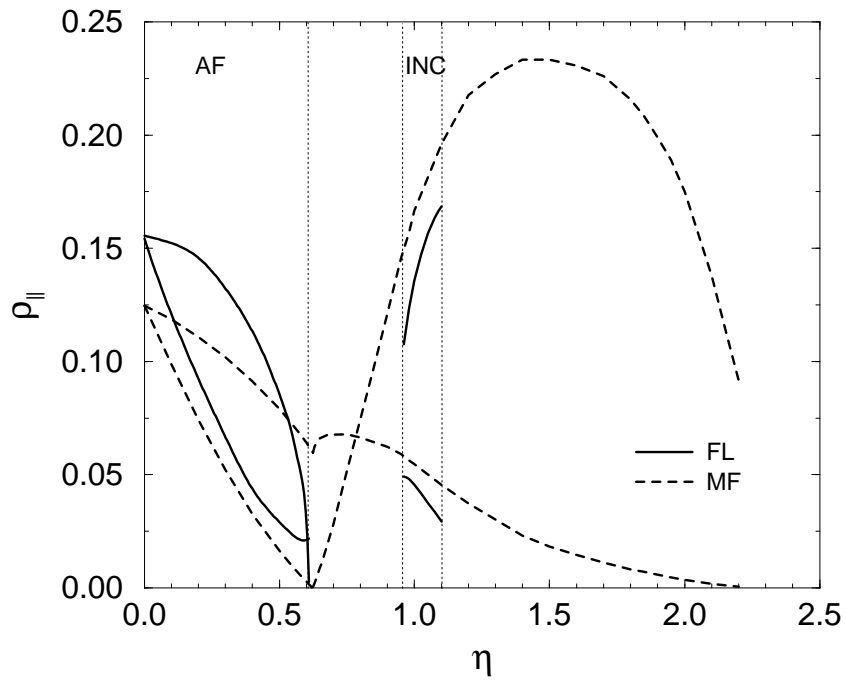


FIG. 5.